

Accumulation mechanism of crust-mantle mixing helium-rich reservoir: A case study of the Subei basin (Eastern China)

Wenqi Li^{a, b, c}, Huichuan Liu^{a, b, *}, Greg Holland^d, Zheng Zhou^c, Jianfa Chen^{a, b}, Jian Li^e, Xiaobo Wang^e,
a. State Key Laboratory of Oil and Gas Resources and Exploration, China University of Petroleum (Beijing), Beijing 102249, China;
b. College of Earth Sciences, China University of Petroleum (Beijing), Beijing 102249, China;
c. Lancaster Environment Centre, Lancaster University, LA1 4YQ, UK
d. Department of Earth and Environmental Sciences, the University of Manchester, M13 9PL, UK
e. Research Institute of Petroleum Exploration and Development, Beijing 100011, China

Abstract:

Helium reservoirs, as an indispensable and scarce strategic resource, can be categorized into two primary origins: crust- and mantle-sourced. Understanding the mechanisms of its formation and accumulation is a crucial challenge in helium exploration. Previous work on helium exploration has mainly focused on crustal helium, while mantle-sourced helium-rich reservoirs have been overlooked. Helium reservoirs with both a crustal and a mantle source exhibit higher helium abundance than that of crustal helium reservoirs and are sporadically distributed in Neogene basins worldwide, but their formation and evolution is poorly understood. In eastern China, several Neogene basins preserve high quality crust/mantle helium-rich reservoirs, and in this study, we use the Subei Basin as a case study to investigate processes controlling He accumulation and storage. The helium reservoirs can be classified into two types based on the lithological nature of the structural traps: sand reservoir with mud cap and basalt reservoirs with mud cap. The main controlling factors for the formation of crust-mantle helium-rich reservoirs include deep-seated faults, magmatic activity, and mineralization of mantle-derived CO₂. Deep-seated faults, along with their associated strike-slip faults, serve as favorable pathways for mantle-derived helium migration and magma

About the author: Li Wenqi (1994–), male, Ph.D. candidate, engaged in rock and noble gas geochemistry research. E-Mail: lwqcup@163.com

Corresponding author: Liu Huichuan(1986–), male, associate professor, doctoral supervisor, mainly engaged in structural geology and rock geochemistry research. E-Mail: lhc@cup.edu.cn

27 upwelling. Magmatic activities serve as the material source for mantle-derived helium
28 as well as the carrier medium in the migration of mantle-derived volatiles. The presence
29 of well-developed sandstone and basalt reservoirs, along with mudstone cap rocks and
30 the dissolution and mineralization caused by mantle-derived CO₂ are important factors
31 in helium accumulation and preservation.

32 Keywords: crust-mantle mixing helium, helium-rich reservoir, ³He/⁴He, accumulation
33 mechanism

34 **1. Introduction**

35 Helium is one of noble gases with special properties: chemical inertness, low
36 boiling point, and low density. It has extensive applications in high-tech fields, such as
37 cryogenic superconductivity, aerospace, nuclear industry, and medical technology
38 therefore helium is regarded as a crucial resource for modern industry (Cai et al., 2010;
39 Chen, et al., 2021). Generally, helium cannot accumulate independently to form
40 reservoirs but is found in association with inorganic or organic gases, existing as part
41 of natural gas reservoir components. Helium in natural gas of sedimentary basins has
42 three sources: the atmosphere, the crust and the mantle. These different sources can be
43 discriminated by their isotope compositions. Helium (He) has two isotopes, with ³He
44 being primordial and ⁴He produced primarily by the decay of uranium and thorium.
45 Atmospheric helium the helium in the air with a concentration of 5.24×10^{-6} , it was
46 mainly produced from volcanic eruption, magma degassing, and rock weathering, with
47 ³He/⁴He of 1.4×10^{-6} , which is referred as 1 Ra (Mamyrin et al., 1970). The helium
48 origin can be determined by ³He/⁴He ratios (R/Ra values), which have been widely used
49 to trace the mantle-derived volatiles (Wakita and Sano, 1983; Oxburgh et al, 1986;
50 Poreda et al, 1988; Xu et al, 1996). R/Ra >1 suggests the input of considerable mantle-
51 derived helium, whereas R/Ra ≤ 0.1 implies mainly crustal helium (Oxburgh et al,
52 1986). Atmospheric helium enters the basin fluid system through groundwater recharge.

53 Crustal helium is predominantly composed of radiogenic ^4He . Meanwhile, mantle-
54 derived helium is primarily from mantle degassing.

55 Worldwide large-scale helium-bearing reservoirs, such as those in the United
56 States, Qatar, Algeria, Russia, and Canada, are predominantly crustal helium (Yakutseni,
57 2014). In contrast to crustal helium reservoirs, which tends to accumulate in stable
58 craton basins, crust-mantle mixing helium-rich reservoirs with both crustal and mantle
59 derived helium are usually found within tectonically and magmatically active regions
60 (Figure 1), such as the active continental margins encircling the Pacific Ocean including
61 the Taupo Arc, the Kurile-Honshu-Ryukyu Arc, the Aleutian-Alaskan Arc, and the
62 western margin of North America. However, the helium content in these reservoirs is
63 not high enough to be economically viable (Poreda et al., 1986, 1988; Motyka et al.,
64 1989). Furthermore, some previously presumed helium reservoirs of mixed crustal and
65 mantle origin within the Rukawa Rift Basin of the East African Rift have been identified
66 as crustal helium origin (Kimani et al., 2021; Mtili et al., 2021). In eastern China,
67 several Neogene basins (such as Songliao, Bohai Bay, Subei and Sanshui basins)
68 preserved crust-mantle mixing helium-rich reservoirs. These basins are distributed in a
69 narrow belt along the active continental margin in western Pacific Ocean, providing an
70 excellent opportunity for studying processes of accumulation, migration, and storage of
71 these types of helium-rich reservoirs (Xu et al. 1996).

72 In comparison to crustal helium reservoirs, Helium-rich reservoirs with a mantle
73 component are characterized by higher helium contents, than those with only crustal
74 source. They also exhibit younger formation period (mainly in Neogene) and occur in
75 active tectonic-magmatic settings. However, the accumulation mechanisms of crust-
76 mantle mixing helium-rich reservoirs remain enigmatic. The Subei Basin is a typical
77 Neogene basin with crust-mantle mixing helium-rich helium accumulations where
78 crust-mantle mixing helium-rich reservoirs have highest helium contents (up to 1.32%)
79 in China. Therefore, we focus on the Subei Basin as a case study for comparison of
80 accumulation and enrichment of helium in both stable cratonic basins and tectonic-

81 magmatic active regions.

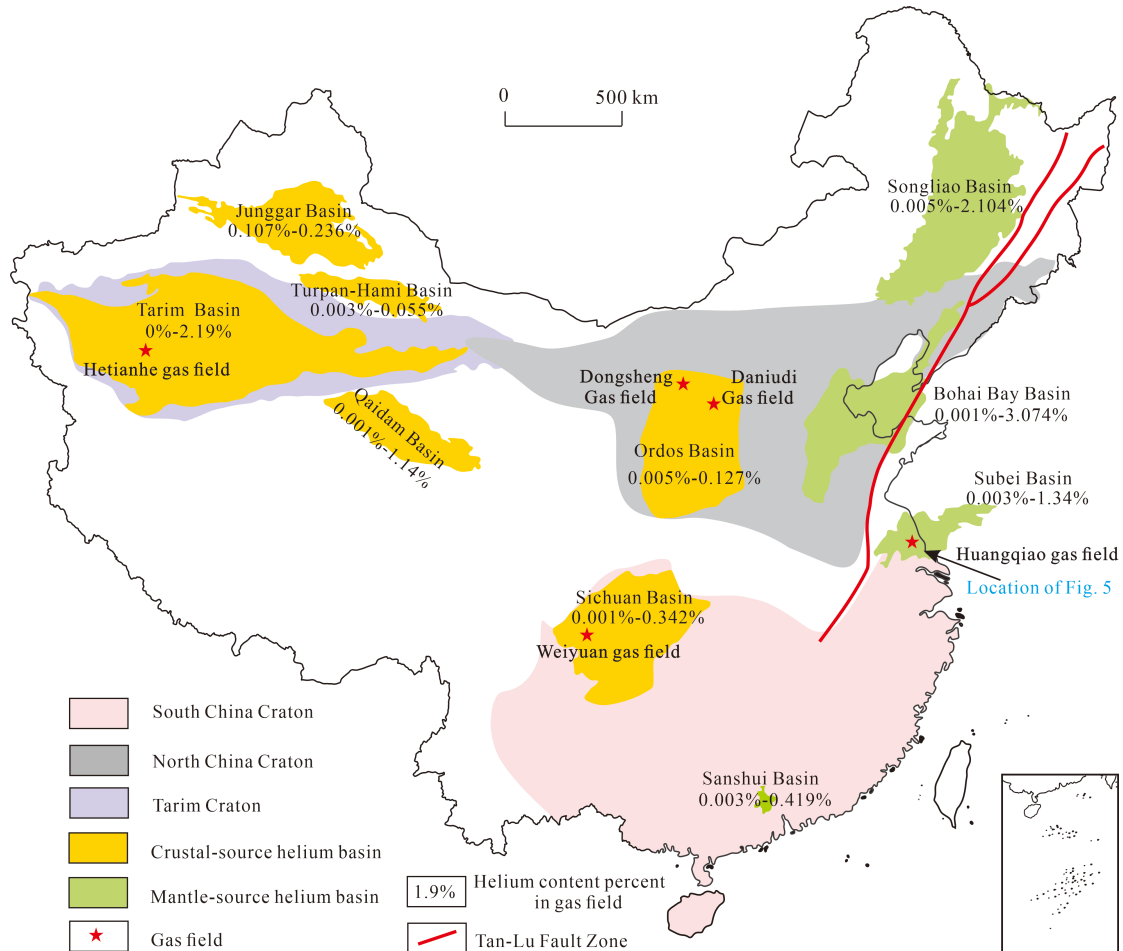


82
 83 Figure 1. Global distribution map of helium resources (modified after Furnes et al., 2015). Helium
 84 date sources are from: Wakita and Sano, (1983); Poreda et al. (1986, 1988); Marty et al. (1989);
 85 Motyka et al. (1989); Merrill et al (2014); Yakutseni (2014); Xu et al. (2017); Mtili et al. (2021);
 86 Halford et al. (2022). The average $^3\text{He}/^4\text{He}$ ratio of MORB (8 Ra) is considered as the end member
 87 for the upper mantle in calculations.

88 **2. Spatiotemporal distribution of worldwide crust-mantle mixing helium-rich**
 89 **reservoirs**

90 Commercial helium systems worldwide primarily have been found in helium-
 91 bearing fields within sedimentary basins (Danabalan, 2017). According to Dai et al.
 92 (2017) classification criteria for helium reservoirs, fields with reserves exceeding
 93 $1.0 \times 10^8 \text{m}^3$ are referred to as extra-large gas fields. Those with reserves ranging from
 94 5.0×10^7 to $1.0 \times 10^8 \text{m}^3$ are classified as large gas fields. Reserves falling between
 95 2.5×10^7 to $5.0 \times 10^7 \text{m}^3$ are termed as medium gas fields, while fields with reserves
 96 between 5.0×10^6 to $2.5 \times 10^7 \text{m}^3$ are categorized as small gas fields. It is generally

97 considered that natural gas reservoirs with helium content below 0.05% are categorized
 98 as helium-depleted gas reservoirs, while those with helium content exceeding 0.1% are
 99 referred to as helium-rich natural gas reservoirs, meeting the threshold for economic
 100 viability.



101
 102 **Figure 2. Distribution of helium resources in China.**

103 Helium data sources are from: Songliao Basin (Xu et al., 1996; Feng et al., 2001; Wang et al., 2006;
 104 Yang et al., 2014), Bohai Bay Basin (Zheng et al., 1996; Cao et al., 2001; Dai et al., 2017; Ni et al.,
 105 2022), Subei Basin (Xu et al., 1996; Guo et al., 1999; Ye et al., 2003; Liu et al., 2017), Sanshui
 106 Basin (Du and Liu, 1991; Dai et al., 1995; Xu et al., 2000), Sichuan Basin (Du and Liu, 1991; Ni et
 107 al., 2014; Wei et al., 2014; Liu et al., 2017), Ordos Basin (Liu et al., 2007; Ni et al., 2010; Dai et al.,
 108 2017), Tarim Basin (Xu et al., 1998; Liu et al., 2009; Liu et al., 2012; Yu et al., 2013; Wang et al.,
 109 2016; Wang et al., 2018; Tao et al., 2019), Qaidam Basin (Cao et al., 2016; Zhang et al., 2016; Xu
 110 et al., 2017), Turpan-Hami Basin (Xu et al., 2017).

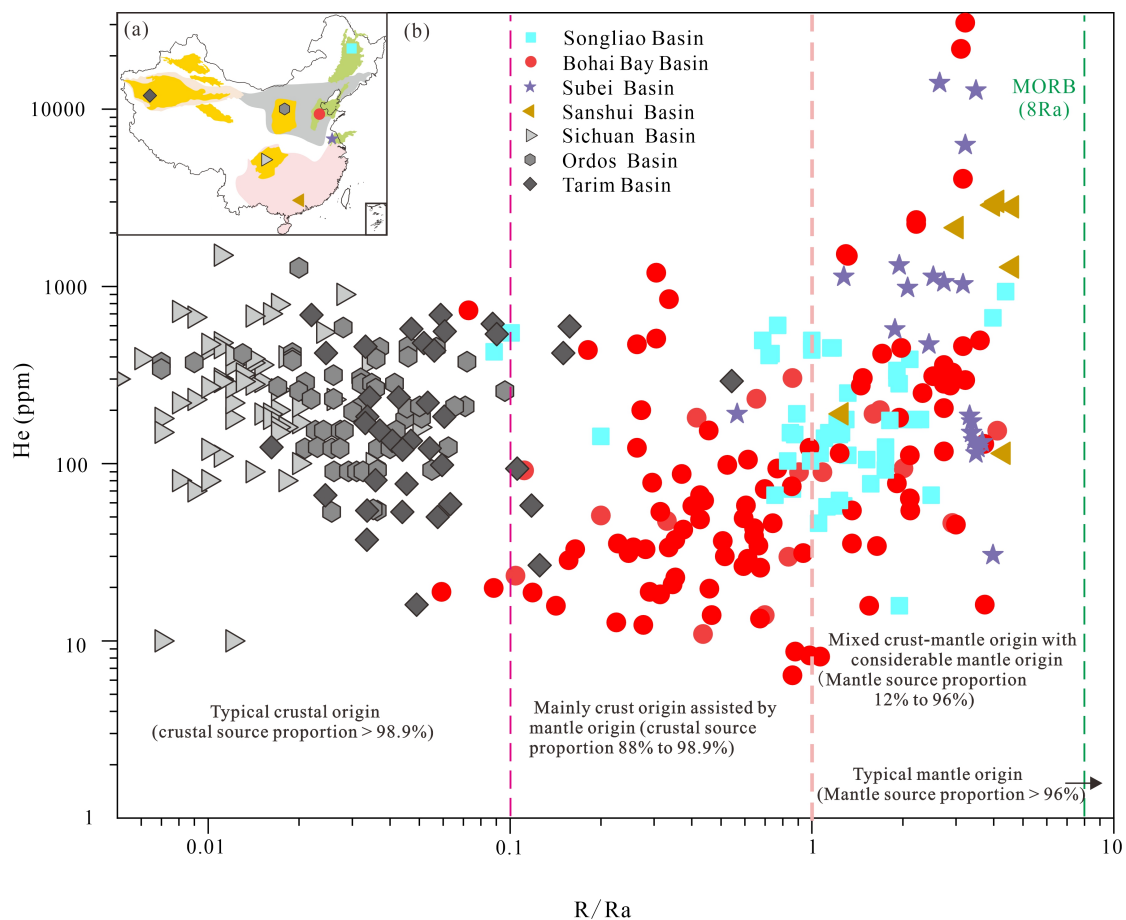
111 Table 1. Global distribution of mantle-derived helium resources. Helium data from: Poreda et al.

Location	Basin	Gas field	Strata	Depth/m	Reservoir	CO ₂ /%	He/%	R/Ra	
New Zealand	Taranaki, North Island	Maui	Paleogene-Neogene	/	Sandstone	4.8	0.0182 (n=1)	3.5	
		Kapuni	Paleogene- Neogene	/	Sandstone	39.2	0.0013 (n=1)	0.19	
Philippines	Palawan	Matinloc <i>P-I</i>	Neogene	2234-2246	Carbonate	5.4	0.0010 (n=1)	0.1	
		Nido BW	Neogene	2051-2103	Carbonate	20	0.0093 (n=1)	3.34	
	/	Chinsui	Neogene	3840-4214	Sandstone	11.2	0.0027 (n=1)	1.55	
	/	Yunghoshan	Neogene	4787-4913	Sandstone	10.9	0.0014 (n=1)	1.65	
	/	Chingtsaohu	Neogene	3861-3870	Sandstone	3.7	0.0034 (n=1)	3.22	
Taiwan, China	/	Tienchenshan	Neogene	2706-3057	Sandstone	2.2	0.0039 (n=1)	1.4	
	/	Chuhuanguan	Neogene	4116-4421	Sandstone	45.3	0.0038 (n=1)	3.4	
	/	Pachangchi	Neogene	1882-1922	Sandstone	0.7	0.0063 (n=1)	1.04	
	/	K-16	/	/	Sandstone	53.9	0.0138 (n=1)	3.84	
	/	K-16	/	/	Sandstone	2.9	0.0072 (n=1)	2.6	
U. S. A	Cook Inlet	McArthur River	Paleogene-	/	Sandstone	0.8	0.0130 (n=1)	0.75	
		Wanjinta	Cretaceous	800-1400	Sandstone	90-99.5	0.07-0.08 (n=4)	4.5-5.1	
China	Songliao Basin	Gulong depression	Saertu Formation	1100-1600	Sandstone			0.9-1.9	
		Daqing Changyuan	Saertu Formation	900-1200	Sandstone			1.32-2.18	
		Sanzhao Depression	Fuyu Formation	1200-1350	Sandstone	0.08-45.2	0.102-0.404 (n=50)	0.72-3.05	
	China	Chaochang	Fuyu Formation	950-1100	Sandstone			1.02-2.06	
		Huangqiao	Yancheng Formation	350-400	Sandstone	15	0.013-1.34 (n=5)	2.65-3.96	
		Subei Basin	Qintong Depression	Yancheng Formation	2300-2600	Sandstone	15.5-92.06	0.089-0.096 (n=3)	2.54-2.74
			Jinhu Depression	Funing Formation	1650	Basalt	0.55	0.10 (n=6)	1.25
Sanshui Basin	/	Paleogene	700-1800	Sandstone	1.45-99.6	0.08-0.26 (n=7)	1.22-4.56		

113 Mantle-derived helium reservoirs worldwide located along the margins of active
114 tectonic plates are generally relatively associated with deep-seated faults and magmatic
115 activity. Mantle-derived helium reservoirs in China show relatively shallow burial
116 depths, averaging between 1 km to 4 km, and are located in the Neogene basins near
117 the Tan-Lu Fault Zone (Figure 2). The Tan-Lu Fault Zone has played an important role
118 in the formation, evolution and the distribution of hydrocarbon-bearing Neogene basins
119 on both sides, as well as in the genesis and distribution of natural gas (Tao et al., 2001).

120 Helium-bearing reservoirs in the Songliao Basin are located in the southeastern
121 and northern areas, including the Wan Jinta gas field, Gulong Depression, Daqing
122 Changyuan, Sanzhao Depression, and Chaolang Platform. In the Wanjinta gas field, the
123 R/Ra values range from 4.5 to 5.1(Xu et al., 1995, 1996). The proportion of mantle-
124 derived helium can reach as high as 57.2% to 65.4%. Furthermore, in Wells Wan 5 and
125 Wan 6, of which the helium contents are 0.07% to 0.08%, approaching industrial helium

126 values. The relatively high proportion of mantle-derived helium in the Wanjinta gas
 127 field may be associated with its structural position, where is in close proximity to the
 128 western side of the Tan-Lu Fault Zone. It is also possible that the Wanjinta gas field is
 129 located directly above an ancient volcanic caldera, leading to the high proportion of
 130 mantle-derived helium (Xu et al., 1996). Mantle-derived helium reservoirs exhibit
 131 burial depths ranging from 589.6 to 3630 meters in northern Songliao Basin. The
 132 helium content typically ranges between 0.102% and 0.404%, with exceptionally high
 133 helium content reaching 2.104% in Wells Wang 9-12. $^3\text{He}/^4\text{He}$ ratios range from 0.1 to
 134 3.0 (Zhong et al., 2017). The mantle-derived helium proportion of northern Songliao
 135 Basin varies in proportion from 1.3% to 38.2%. Specifically, the Gulong Depression
 136 (11.1%-24%), Daqing Changyuan (16.9%-27.7%) and Sanzhao Depression (9.1%-
 137 38.2%), which exhibit relatively higher proportions of mantle-derived helium. In
 138 contrast, the Chaolang Platform (1.3%-2.6%) has a relatively lower proportion of
 139 mantle-derived helium.



141 Figure 3. Genesis types of helium in Chinese sedimentary basins. Helium data sources are the
142 same as in Figure 2. The average $^3\text{He}/^4\text{He}$ ratio of MORB (8 Ra) is considered as the end member
143 for the upper mantle in calculations.

$$144 \quad R/Ra = (^3\text{He}/^4\text{He})_{\text{sample}} / (^3\text{He}/^4\text{He})_{\text{atmosphere}}$$

$$145 \quad \text{Helium}_{\text{mantle}} (\%) = [(^3\text{He}/^4\text{He})_{\text{sample}} - (^3\text{He}/^4\text{He})_{\text{crust}}] / [(^3\text{He}/^4\text{He})_{\text{mantle}} - (^3\text{He}/^4\text{He})_{\text{crust}}] * 100$$

146 Helium-bearing reservoirs in the Bohai Bay Basin have been found in the Jiyang,
147 Dongpu and Huanghua depressions. The helium contents of natural gas from the Bohai
148 Bay Basin range from 0.0005% to 0.26% with an average of 0.0197% (Zhang et al.,
149 2008; Dai et al., 2017). The R/Ra ratios of natural gas from the Bohai Bay Basin range
150 from 0.059 to 3.74 with an average of 1.013, indicating general mixing of mantle-
151 derived helium by various degrees (Zhang et al., 2008; Dai et al., 2017; Figure 3).
152 Natural gas from the Dongpu Sag has the helium contents ranging from 0.0031% to
153 0.0217% averaging 0.0133% (Ni et al., 2022). The R/Ra ratios of natural gas from the
154 Dongpu Sag range from 0.011 to 0.856, the proportion of mantle-derived helium in the
155 gas ranges from 0.01% to 10.72% with an average of 2.39%, displaying the
156 characteristics of mixing between crustal and mantle-derived helium.

157 The Sanshui Basin is a Cenozoic to Neogene basin, located in the western part of
158 the Pearl River Delta, with an area of 3380 km². During the Cretaceous to Paleogene,
159 the Sanshui Basin experienced intense volcanic activity, with magma events primarily
160 controlled by the intersecting extensional faults oriented in the northeast and northwest
161 directions. The R/Ra ratio is from 1.22 to 4.56 in the Sanshui Basin. The mantle-derived
162 helium proportion constitutes 15.6% to 58.1%, with an average value of 43%. Among
163 the eight industrial wells tested for helium content, six wells have helium concentrations
164 that meet industrial helium values, ranging from 0.085% to 0.259% (Xu et al., 1996).

165 3. Accumulation conditions of helium reservoir in Subei Basin

166 3.1 Helium sources

167 Natural gas of the Subei Basin is composed of C₁-C₅ alkane gas, CO₂, N₂, and
168 trace noble gases. The helium concentration in natural gas varies greatly from 13 to
169 13400 ppm. Helium-rich natural gases in the Subei Basin are primarily located in the
170 Huangqiao gas field, the Qintong Depression and the Jinhu Depression (Xu et al., 1996).
171 Huangqiao gas field is mainly composed of N₂, CH₄ and CO₂, with N₂ contents
172 exceeding 56%. The CH₄ and CO₂ contents are approximately 24% to 28% and around
173 15%, respectively. The He contents range from 0.013% to 1.34%, with highest contents
174 of 1.34% in the Huangqian 14 well (Yang et al., 1991). In the Qintong Depression, Well
175 Su203 is rich in CO₂ with a concentration of 92.06%, and the He concentration is
176 0.089%. In Well Su190, N₂ is predominant at 33.07%, and the helium concentration is
177 0.096%. The helium contents in the Jinhu Depression range from 0.081% to 0.096%,
178 essentially meeting industrial helium value. In the Subei Basin both hydrocarbon and
179 non-hydrocarbon natural gases could be helium enriched as shown in Figure 4(a).
180 Helium contents show positive correlation with N₂ levels, but variable correlation with
181 CO₂ contents. Main reason for such correlations and some low CO₂ contents is that the
182 mineralization of CO₂ leading to the dissolution of minerals in reservoir such as feldspar
183 and chlorite and self-sealing effect in the cap rock caused the loss of mantle-derived
184 CO₂, which will be discussed in section 3.3.

185

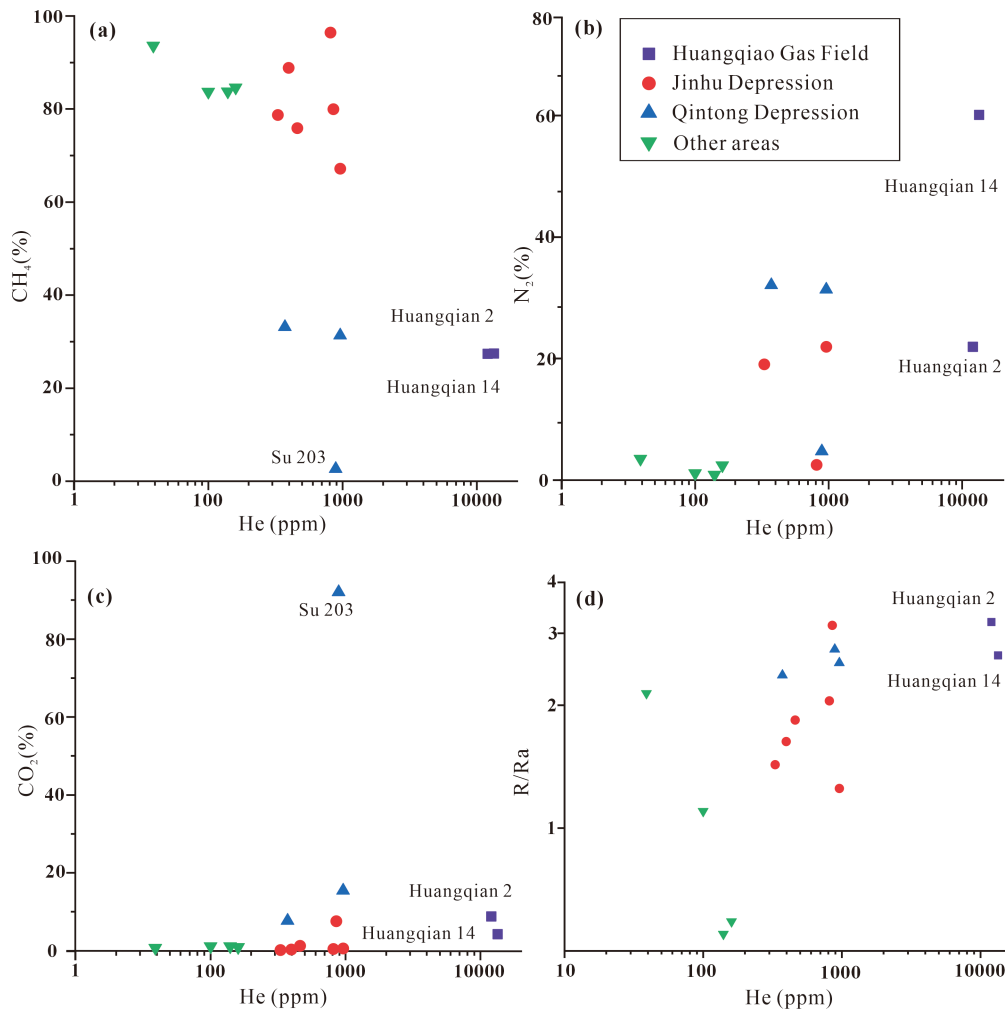


Figure 4. Chemical composition of natural gas in Subei Basin.

186

187

188 Helium data sources are from Xu et al. (1996); Yang et al. (1991); Dai et al. (1994); Tao et al.
 189 (1997); Guo et al. (1999). The average $^3\text{He}/^4\text{He}$ ratio of MORB (8 Ra) is considered as the end
 190 member for the upper mantle in calculations.

191 The three different sources (atmosphere, crust, and mantle) of helium in natural
 192 gases could be discriminated by their $^3\text{He}/^4\text{He}$ ratios (Ballentine and O’Nions, 1992).
 193 $^3\text{He}/^4\text{He}$ ratios of atmosphere and crust have been identified to be 1.4×10^{-6} and $2.0 \times$
 194 10^{-8} , respectively. However, $^3\text{He}/^4\text{He}$ ratio of the mantle remains controversial as the
 195 Earth’s mantle is chemically and isotopically heterogeneous (Wang et al., 2022). For
 196 example, mid-ocean ridge basalts, formed by melting of the upper mantle, demonstrate
 197 a relatively consistent $^3\text{He}/^4\text{He}$ ratio, with an average value of 8 ± 1 Ra, reflecting the
 198 composition of the upper mantle (Allègre et al., 1995). By comparison, ocean island
 199 basalts formed at intraplate volcanic hotspots, believed to be melts from buoyant mantle

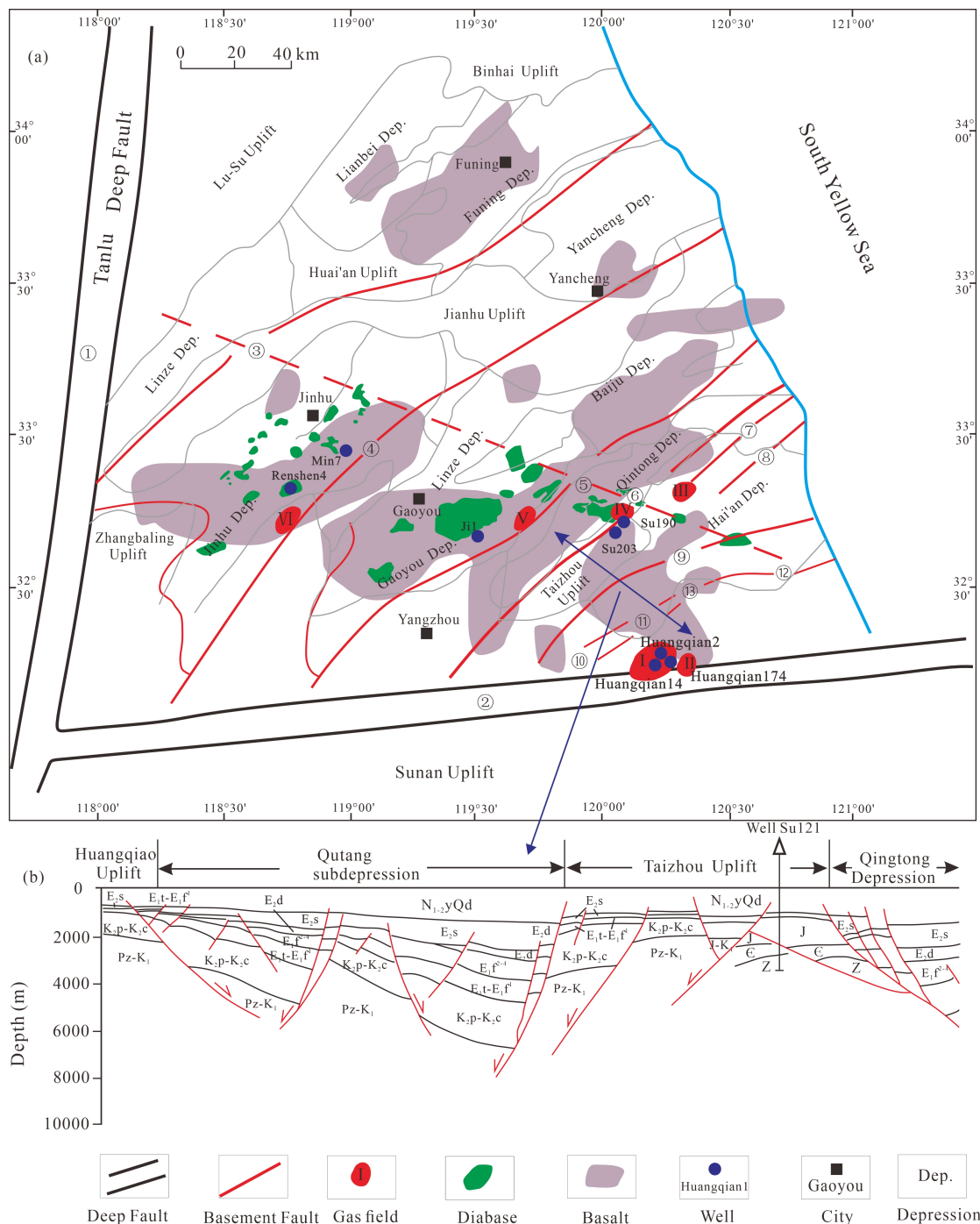
200 plumes originating in the deep mantle, erupt lavas with $^3\text{He}/^4\text{He}$ ratios ranging from 4
201 to 42.9 Ra (Moreira et al., 1999). In addition, olivine phenocrysts and xenoliths in
202 samples from the sub-continental lithosphere mantle (SCLM) show a homogeneous
203 helium isotopic ratio ($R/\text{Ra}=6.1\pm 0.9$) (Gautheron and Moreira, 2002). The
204 heterogeneity of the mantle is mainly caused by metasomatism of subducted oceanic
205 crust (Ma et al., 2006; Dai et al., 2019). The Subei basin in eastern China are located in
206 active continental margin of western Pacific Ocean, and sub-continental mantle in
207 Subei basin has been severely metasomatized by subducted oceanic crust (Wang et al.,
208 2022). Mantle xenoliths in different regions of eastern China exhibit variable $^3\text{He}/^4\text{He}$
209 ratios, which are notably lower than those of typical MORB and OIB (Xu et al., 1995;
210 Lai et al., 2002; Li et al., 2002; Ma et al., 2006). The $^3\text{He}/^4\text{He}$ ratio of metasomatized
211 mantle xenoliths in eastern China has been reported to be 5 Ra (Lai et al, 2002), so we
212 use this ratio as the end member for mantle-derived helium in our mixing calculations.
213 The $^3\text{He}/^4\text{He}$ ratios of natural gas in Subei Basin has a range of 0.55-3.2 Ra (Figure
214 4(d)), an average 1.95 Ra, resulting in the contribution of mantle-derived helium
215 ranging from 10% to 78%, with an average of 40.1%. Previous studies by Xu et al.
216 (1998) and Wang et al. (2022) calculated the ratios of mantle helium contribution to be
217 10% to 60%, with an average of 34.6% due to use of typical MORB as the mixing
218 endmember of the mantle.

219 The average contribution of mantle-derived helium is 40.1% with the remainder
220 (59.9%) assumed to be crustal in origin. This reflects the addition of radiogenic helium
221 to the mantle derived helium during magma ascent. The R/Ra ratio show positive
222 correlations with the helium contents (Figure 4(d)) supports the idea of magmatic
223 helium with a crustal addition.

224 **3.2 Migration of mantle-derived helium**

225 During the process of helium migration, deep-seated faults serve as the primary
226 conduit for the ascending mantle-derived helium. As the deep-seated faults cut through

227 the lithospheric mantle, they provide favorable migration paths for mantle-derived
 228 volatiles. These deep-seated faults effectively connect reservoirs in both vertical and
 229 planar dimensions through secondary faults derived in the shallow subsurface (Wang,
 230 et al., 2008). Moreover, magmatic activity can facilitate the upward migration of
 231 mantle-derived helium through deep-seated faults (Tao et al., 1996, 2001). Similarly,
 232 migration of crustal helium to shallow sedimentary layers is dependent on basement
 233 faults.



235 Figure 5. Fault system and distribution of major mantle-derived gas fields in the Subei Basin
236 (modified from Wang et al., 2008 and Luo et al., 2011).

237 (I Huangqiao gas field; II Xiqiao gas field; III Anfeng gas field; IV Hongzhuang CO₂ gas field;
238 V Xiaoji CO₂ gas field; VI Tianchang-Tianshen 1 Well CO₂ gas field; ① Tanlu Fault; ② Along the
239 Yangtze Fault; ③ Hongze-Funing Fault; ④ Tianchang-Liupu West Fault; ⑤ Gaolizhuang-Xiaoji
240 Fault; ⑥ Qintong Fault; ⑦ Liangduo Fault; ⑧ Fuan Fault; ⑨ Zhangjiaduo-Beiling Fault; ⑩
241 Nanxinjie Fault; ⑪ Tazili Fault; ⑫ Lifa-Xichang Fault; ⑬ Yazhou Fault).

242 The western boundary of the Subei Basin closely abuts the Tan-Lu Fault Zone,
243 while the southern margin is defined by the Jiangnan Fault. Both faults traverse the
244 lithospheric mantle, effectively connecting with the mantle-derived helium source and
245 serving as conduits for the migration of mantle-derived helium (Xu et al., 1996; Wang
246 et al., 2008; Figure 5(a)). The basement faults, as shown in Figure 5(b), serve as
247 favorable migration paths for crustal helium. The Huangqiao gas field is located closely
248 to the Jiangnan Fault. Multiple significant basement faults with a north-northeast and
249 north-northeast to east-northeast orientation have been discovered in the Neogene strata.
250 The Jiangnan Fault and these basement faults, potentially branches of the Jiangnan
251 Fault, are considered as the primary controlling faults for the communication of mantle-
252 derived helium and crustal helium in the Huangqiao slope (Cao et al., 2021).

253 Mantle-derived helium gas and Neogene magmatic activity are closely associated
254 in extensional tectonic regions (Sano et al., 1984; O'Nions and Oxburgh, 1988;
255 Kennedy and van Soest, 2006). Mantle sourced magma serves as the carrier for the
256 reservoir and migration of deep-seated gas source. Magmatic activities are widespread
257 in eastern China during the Neogene. In the Subei Basin, Neogene magmatic activities
258 are characterized by three rock types, basalt, diabase and gabbro, and three distinct
259 episodes, at approximately 64.5–54.6 Ma, 49.4–39.2 Ma, and 36.7–28.1 Ma. These
260 magma activities align closely with the gas reservoir formation periods in the
261 Huangqiao gas field (as mentioned in section 3.1), being slightly earlier than the
262 accumulation periods.

263 The deep-seated faults and branched basement faults effectively connect the
264 shallow helium reservoirs with the deep mantle and crust (Wang et al., 2008). Moreover,
265 magmatic activity can facilitate the upward migration of mantle-derived helium through
266 deep-seated faults (Tao et al., 1996, 2001). Deep-seated faults and magmatic activity
267 serve as principal determinants in the migration process of mantle-derived and crustal
268 helium.

269 **3.3 Reservoir and seal conditions of crust-mantle mixing helium accumulation.**

270 The chemical inertness and high diffusivity of helium requires the preservation
271 conditions to be more stringent. This includes both the reservoir conditions and the
272 sealing conditions of the cap rock.

273 The reservoir lithologies of helium-bearing reservoirs in the Subei Basin are
274 primarily sandstone reservoirs with mudstone caps and basalt reservoirs with shale caps.
275 The Huangqiao gas field and the Qintong Depression are mainly characterized by
276 sandstone reservoirs from the Yancheng Formation. In the Jinhu Depression, the
277 reservoirs consist of the upper part of the Funing Formation and the middle part of the
278 second section, mainly comprising olivine basalt.

279 The Huangqiao Slope and the Qintong Depression consist of sandstone reservoirs
280 with mudstone caps. The gas reservoir exhibits a favorable logging response, with gas-
281 bearing characteristics of high porosity and sonic time difference (Figure seen in
282 Supplemental data): In Well Huangqian1, the log response of gas-bearing layer shows
283 high resistivity, a porosity curve with gas-bearing characteristics, an induction
284 resistivity of 12.5 ohms, a sonic time difference of 520 microseconds/m (significantly
285 higher than the non-gas-bearing layers above and below), and a porosity of 43%(Guo
286 et al., 1999). Well Min 7 is located in the Minqiao gas field within the Jinhu Depression.,
287 with reservoirs of the upper section of the Funing Formation consisting predominantly
288 of olivine basalt, including vesicular basalt, amygdaloidal basalt, and dense basalt
289 (Zhang et al., 2001).

290 The properties of the cap rock are crucial in determining whether natural gas can
291 be efficiently accumulated or not. For an efficient natural gas reservoir, the thickness
292 of direct cap rock should exceed 100 meters, and the cap rock capillary pressure should
293 not be less than 20 MPa. In the Subei Basin, the caprock of the Lower Yancheng is
294 composed of mudstone with a thickness ranging from 60 to 100 meters. The
295 breakthrough pressure is suggested to exceed 12 MPa (Sun et al., 2008). The thickness
296 of cap rock within helium-bearing reservoirs in the Subei Basin does not meet the
297 criteria for an efficient cap rock, and the sealing integrity required for helium is even
298 more stringent compared to conventional natural gas implying the preservation of
299 helium need other important factors.

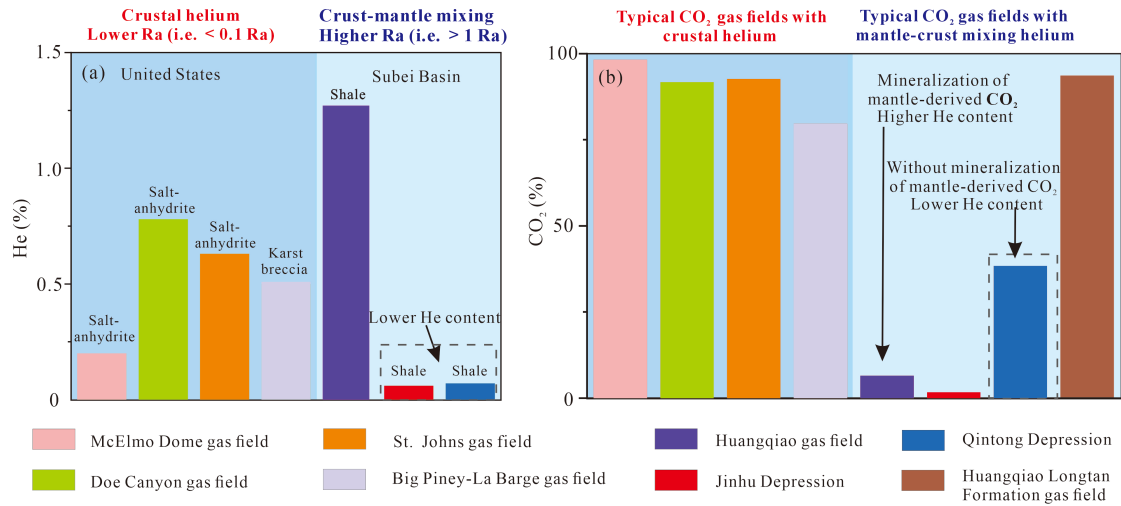
300 In addition, the dissolution and mineralization caused by injection of mantle-
301 derived CO₂ plays an important role in the enrichment and preservation of helium.
302 Mantle-derived CO₂ fluids enter the reservoir along the pathways of the deep-seated
303 fault and fault systems, undergoing physical and chemical reactions through CO₂-
304 water-rock interactions. After mantle CO₂ fluids enters the reservoir, it dissolves in
305 water to form carbonic acid, providing a substantial amount of H⁺ and HCO₃⁻, leading
306 to the dissolution of minerals such as feldspar and chlorite. This process generates a
307 certain quantity of ions such as Ca²⁺, Mg²⁺, Fe²⁺ and AlO₂⁻ (Liu, et al., 2017; Xu et al.,
308 2019). Due to the abundant presence of CO₃²⁻ and HCO₃⁻ ions in the fluid system, ions
309 such as Ca²⁺, Mg²⁺, Fe²⁺, and AlO₂⁻ react with them, resulting in the precipitation of
310 new minerals, which including illite, calcium montmorillonite, albite, siderite, and
311 calcite (Gao et al., 2005, 2007; Yang et al., 2014).

312 In the high-temperature reservoir zone near the fault, where the CO₂ partial
313 pressure is higher, the formation fluids are acidic. In this setting, feldspar dissolves,
314 giving rise to minerals such as albite, kaolinite, and secondary quartz. On the other hand,
315 in the cap rock above the reservoir, which is in the medium-low-temperature zone and
316 experiences lower CO₂ partial pressure, the formation fluids undergo a transition from
317 acidity to neutral to weak alkalinity. This results in the formation of substantial

318 carbonate minerals, such as calcite, siderite, and ankerite, within the fractures of the cap
319 rock, leading to cementation and sealing of the cap rock and further reducing its
320 permeability (Zhang, 2017; Liu et al., 2023). Numerical simulations of the filling and
321 sealing of calcite veins in the cap rock of the Huangqiao gas field indicate that after a
322 simulation time of 0.01 million years, the permeability of the cap rock with calcite-
323 filled fractures has decreased by four orders of magnitude compared to the cap rock
324 permeability before CO₂ fluid intrusion (Xu et al., 2019).

325 By the comparison of helium-rich gas fields in Subei Basin with those in the
326 United States (Figure 6(a)), the results show that the helium-rich CO₂ gas fields in the
327 United States have higher He content as salt-anhydrite shows better sealing integrity
328 than shale and mudstone. However, the Helium content of Huangqiao gas field is much
329 higher than that of other gas field, indicating that the lithology of caprock not the
330 controlling factor influencing the sealing of caprock. In addition, by the contrast of the
331 CO₂ content of different gas fields (Figure 6(b)), the CO₂ content of shallow Huangqiao
332 gas field is extremely low, while the CO₂ content of deeper Huangqiao gas field in
333 Longtan formation is over 90%. We infer that the dissolution and mineralization of
334 mantle CO₂ contributes to the sealing of caprock.

335 The intrusion of deep-seated CO₂ fluids into the reservoir and overlying cap rock
336 leads to dissolution of minerals in the reservoir and a self-sealing effect in the cap rock
337 through CO₂-water-rock reactions. Dissolution of existing minerals consumes CO₂,
338 reduces the concentration of CO₂ in the reservoir which has the effect of enriching the
339 proportion of mantle-derived helium. The self-sealing effect further reduces the
340 permeability of the cap rock, allowing the helium to be preserved effectively. The self-
341 sealing effect induced by the intrusion of CO₂ fluids is a key factor influencing the
342 preservation conditions of helium accumulation.



343

344 Figure 6. The comparison of helium-rich gas fields in Subei Basin with Colorado Plateau United
 345 States. (a) The relationship between He content and the lithography of the caprock. (b) The CO₂
 346 content of the different gas fields. Helium data sources are from: Xu et al. (1996); Guo et al. (1999);
 347 Ye et al. (2003); Liu et al. (2017); Nichols et al. (2014); Tedesco (2022).

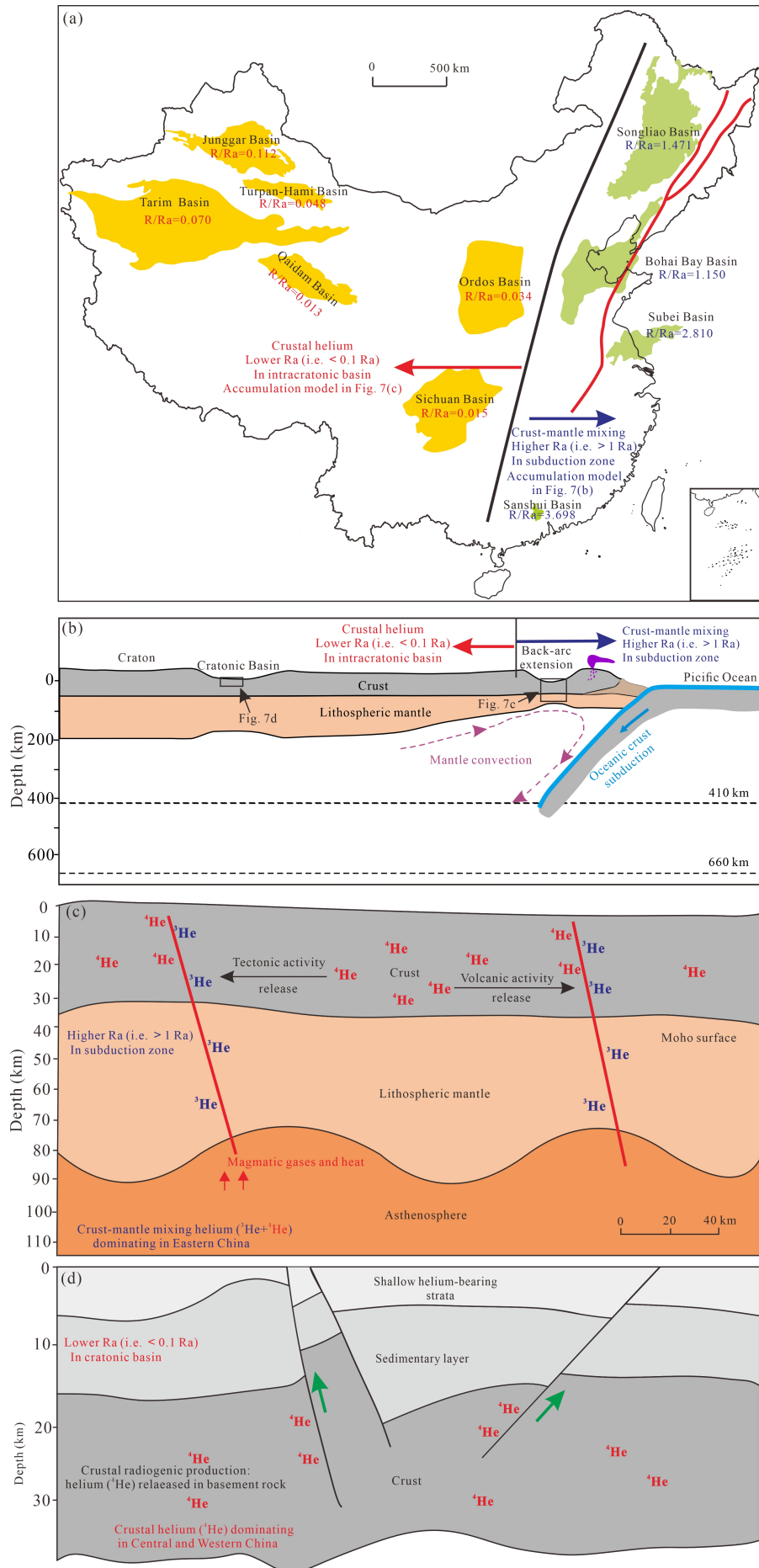
348 4. The mechanism of crust-mantle mixing helium accumulation

349 Crust-mantle mixing helium reservoirs in eastern China are formed in a rift
 350 environment characterized by specific tectonic features. These features include mantle
 351 upwelling, thinning of the crust, extensive development of faults, long-term inheritable
 352 activity of lithospheric faults connecting the upper mantle to the shallow subsurface,
 353 and high geothermal gradients favorable for the migration of mantle-derived helium
 354 (Tao et al., 1997).

355 Figure 7(a, b) shows the regional differences across China in terms of crustal vs
 356 mantle He sources. The crust-mantle mixing helium is mainly distributed in back-arc
 357 basins of subduction zone of Eastern China, with the characteristic of higher Ra value
 358 (i.e. > 1 Ra). While the crustal helium is predominantly distributed in intracratonic
 359 basins of Central and Western China, with the characteristic of lower Ra value (i.e. <
 360 0.1 Ra). The tectonic environments of crust-mantle mixing helium and crustal helium
 361 exhibit significant differences corresponding to the sources of helium (Figure 7(b)).

362 In Eastern China, Mantle fluids and basaltic magma carried helium migrating
363 directly upward through the deep-seated fault, entering traps and accumulating through
364 branches and derivative strike-slip faults of the deep-seated fault in the shallow
365 subsurface (Figure 7(c)). By contrast, the crustal helium was being stored within U-Th-
366 rich crustal rocks and released during tectonic events in Central and Western China.
367 The migration paths are depended on basement faults. The crustal helium can be
368 migrated to the shallow sedimentary layers through basement faults during tectonic
369 activities (Figure 7(d)).

370 Generally, helium is commonly associated with natural gas reservoirs. Therefore,
371 the accumulation of helium in the gas reservoirs depends on the charging episodic
372 periods of natural gas. Taking the Huangqiao gas field as an example, the inorganic gas
373 reservoirs in the Subei Basin generally underwent three phases of charging and
374 reservoir formation processes (Wang et al., 2008). The first phase occurred in the early
375 Late Cretaceous period (90 Ma), was primarily characterized by the charging and
376 reservoir formation dominated by oil and gas. The second phase, transpiring around the
377 Paleogene period (60 Ma), was characterized by dominant oil and gas charging,
378 accompanied by the phenomenon of CO₂ migration and accumulation. The third phase,
379 taking place in the Neogene period (25 Ma), involved CO₂ charging, displacing the
380 hydrocarbons formed in the early stages, which corresponds to the formation period of
381 the Xiqiao gas reservoirs. The deep CO₂ reservoirs in the Huangqiao gas field
382 experienced multiple phases of accumulation, with deposition periods occurring during
383 the Paleogene (60 Ma) and the Neogene (25 Ma) epochs, respectively (Wang et al.,
384 2008). Inclusion data indicates that the formation period of helium-bearing CO₂
385 reservoirs occurred later than the period of oil and gas reservoir formation, primarily
386 during the Paleogene to Neogene, approximately 25 Ma. The main period of oil and gas
387 reservoir formation took place during the Late Cretaceous (90 Ma) in the late Yanshan
388 period, while the Xishan period (25 Ma) witnessed the accumulation of mantle-derived
389 helium.



391 Figure 7. A schematic conceptual model illustrating the regional differences across China in
392 terms of crustal vs mantle He sources. (a) The horizontal regional differences between Eastern China
393 and Central and Western China in terms of crustal vs mantle He sources. (b) The differences of
394 tectonic environments between Eastern China and Central and Western China. (c) Crust-mantle
395 mixing helium dominating in Eastern China. (d) Crustal helium dominating in Central and Western
396 China. Helium data sources are the same as in Figure 2. The average $^3\text{He}/^4\text{He}$ ratio of MORB (8 Ra)
397 is considered as the end member for the upper mantle in calculations.

398 The main controlling factors for the formation of crust-mantle mixing helium
399 reservoirs include deep-seated faults, magmatic activity, and mineralization of mantle-
400 derived CO_2 . Deep-seated faults, along with their associated strike-slip faults, serve as
401 favorable pathways for magma upwelling and mantle-derived helium migration.
402 Magmatic activities serve as the material source for mantle-derived helium as well as
403 the carrier medium in the migration of mantle-derived volatiles. The presence of well-
404 developed sandstone and basalt reservoirs, along with mudstone cap rocks and the
405 dissolution and mineralization of mantle-derived CO_2 are considered to be dominant
406 mechanisms for mantle-derived helium accumulation and preservation.

407 **5. Conclusion**

408 (1) The helium in the Subei Basin is derived from a crust-mantle mixed source.
409 The average contribution of mantle-derived helium is about 40.1%, which is higher
410 than that of previous studies, based on our new calculating method using the new
411 mixing endmember of the mantle.

412 (2) The main controlling factors for the accumulations of mantle-derived helium
413 include deep-seated faults, magmatic activity, and mineralization of mantle-derived
414 CO_2 .

415 (3) The dissolution and mineralization of mantle-derived CO_2 are considered to be
416 predominant mechanisms for mantle-derived helium accumulation and preservation.

417 **Acknowledgments**

418 We thank the editor for handling this manuscript and reviewers for helpful
419 comments and suggestions that have improved the manuscript.

420 **Disclosure statement**

421 No potential conflict of interest was reported by the author(s).

422 **Funding**

423 This work was financially supported by National Key Research and Development
424 Program of China (2021YFA0719000), and China Sponsorship Council
425 (202306440071).

426 **References**

- 427 Allègre, C. J., Moreira, M., and Staudacher, T., 1995, $^4\text{He}/^3\text{He}$ dispersion and mantle convection:
428 Geophysical Research Letters, v. 22, no. 17, p. 2325-2328.
- 429 Ballentine, C. J., and Burnard, P. G., 2002, Production, release and transport of noble gases in the
430 continental crust: Reviews in Mineralogy & Geochemistry, v. 47, no. 1, p. 481-538.
- 431 Ballentine, C. J., and O'Nions, R. K., 1992, The nature of mantle neon contributions to Vienna Basin
432 hydrocarbon reservoirs: Earth and Planetary Science Letters, v. 113, no. 4, p. 553-567.
- 433 Burnard, P., Bourlange, S., Henry, P., Geli, L., Tryon, M., Natal'In, B., Sengör, A., Özeren, M., and
434 Çagatay, M., 2012, Constraints on fluid origins and migration velocities along the Marmara
435 Main Fault (Sea of Marmara, Turkey) using helium isotopes: Earth and Planetary Science
436 Letters, v. 341, p. 68-78.
- 437 Cai, Z., Clarke, R. H., Glowacki, B. A., Nuttall, W. J., and Ward, N., 2010, Ongoing ascent to the
438 helium production plateau--Insights from system dynamics: Resources Policy, v. 35, no. 2, p.
439 77-89.
- 440 Cao, J., Li, D., and Wang, H., 2021, Analysis and considerations on the relationship between strike-
441 slip faults and non-hydrocarbon gas migration and accumulation in Huangqiao area:
442 Geophysical Prospecting for Petroleum, v. 60, no. 5, p. 149-155.
- 443 Chen, J., Liu, K., Dong, Q., Wang, H., Luo, B., and Dai, X., 2021, Research status of helium
444 resources in natural gas and prospects of helium resources in China: Natural Gas Geoscience,
445 v. 32, no. 10, p. 1436-1449.
- 446 Dai, J., Ni, Y., Qin, S., Huang, S., Gong, D., Liu, D., Feng, Z., Peng, W., Han, W., and Fang, C.,
447 2017, Geochemical characteristics of He and CO₂ from the Ordos (cratonic) and Bohai Bay (rift)
448 basins in China: Chemical Geology, v. 469, p. 192-213.
- 449 Dai, H., Zheng, J., O' Reilly, S., Griffin, W., Xiong, Q., Xu, R., Su, Y., Ping, X. and Chen, F., 201
450 9. Langshan basalts record recycled Paleo-Asian oceanic materials beneath the northwest Nor

451 th China Craton. *Chemical Geology*, v.524, p.88-103

452 Danabalan, D., 2017, Helium: Exploration Methodology for a Strategic Resource [Doctor: Durham
453 University.

454 Deng, J., and Du, Z., 2023, Primordial helium extracted from the Earth's core through magnesium
455 oxide exsolution: *Nature Geoscience*.

456 Doğan, T., Sumino, H., Nagao, K., and Notsu, K., 2006, Release of mantle helium from forearc
457 region of the Southwest Japan arc: *Chemical Geology*, v. 233, no. 3, p. 235-248.

458 Doğan, T., Sumino, H., Nagao, K., Notsu, K., Tuncer, M. K., and Çelik, C., 2009, Adjacent releases
459 of mantle helium and soil CO₂ from active faults: Observations from the Marmara region of
460 the North Anatolian Fault zone, Turkey: *Geochemistry, Geophysics, Geosystems*, v. 10, no. 11,
461 p. Q11009.

462 Du, J., and Liu, W., 1991, The helium and Argon isotopic geochemistry analysis in natural gas in
463 Sanshui Basin: *Natural Gas Geoscience*, v. 6, p. 283-285.

464 Feng, Z., Huo, Q., and Wang, X., 2001, A study of helium reservoir formation characteristic in the
465 North part of Songliao Basin: *Nature gas Industry*, v. 21, no. 5, p. 27-30.

466 Fu, X., and Song, Y., 2005, Inorganic gas and its resource in Songliao Basin: *Acta Petrolei Sinica*,
467 v. 26, p. 23-28.

468 Furnes, H., Dilek, Y., and de Wit, M., 2015, Precambrian greenstone sequences represent different
469 ophiolite types: *Gondwana Research*, v. 27, no. 2, p. 649-685.

470 Gao, Y., Liu, L., and Qu, X., 2005, Dawsonite from Wuerxun Depression in Halaer Basin and its
471 Implication: *Geological Science and Technology Information*, v. 24, p. 45-50.

472 Gao, Y., Liu, L., Yang, H., You, L., and Liu, N., 2007, Characteristics and origin of dawsonite in
473 Gudian carbon dioxide gas field of Songliao Basin: *Acta Petrolei Sinica*, v. 28, p. 62-67.

474 Gautheron, C., and Moreira, M., 2002, Helium signature of the subcontinental lithospheric mantle:
475 *Earth and Planetary Science Letters*, v. 199, no. 1, p. 39-47.

476 Guo, N., You, X., and Xu, J., 1999, Geological character of Xiqiao helium-bearing gas field and
477 prospecting of helium-bearing natural gas in North Jiangsu basin: *Petroleum exploration and
478 Development*, v. 26, no. 5, p. 24-26.

479 Halford, D. T., Karolytè, R., Barry, P. H., Whyte, C. J., Darrah, T. H., Cuzella, J. J., Sonnenberg, S.
480 A., and Ballentine, C. J., 2022, High helium reservoirs in the Four Corners area of the Colorado
481 Plateau, USA: *Chemical Geology*, v. 596, p. 120790.

482 Hu, W., Lu, X., and Fan, M., 2019, Advances in the research of shale caprocks: type, micropore
483 characteristics and sealing Mechanisms: *Bulletin of Mineralogy Petrology and Geochemistry*,
484 v. 38, p. 885-896.

485 Kennedy, B. M., Kharaka, Y. K., Evans, W. C., Ellwood, A., DePaolo, D. J., Thordsen, J., Ambats,
486 G., and Mariner, R. H., 1997, Mantle Fluids in the San Andreas Fault System, California:
487 *Science*, v. 278, no. 5341, p. 1278-1281.

488 Kennedy, B. M., and van Soest, M. C., 2006, A helium isotope perspective on the Dixie Valley,
489 Nevada, hydrothermal system: *Geothermics*, v. 35, no. 1, p. 26-43.

490 Kimani, C. N., Kasanzu, C. H., Tyne, R. L., Mtili, K. M., Byrne, D. J., Kazimoto, E. O., Hillemonds,
491 D. J., Ballentine, C. J., and Barry, P. H., 2021, He, Ne, Ar and CO₂ systematics of the Rungwe
492 Volcanic Province, Tanzania: Implications for fluid source and dynamics: *Chemical Geology*,

493 v. 586, p. 120584.

- 494 Lages, J., Rizzo, A. L., Aiuppa, A., Robidoux, P., Aguilar, R., Apaza, F., and Masias, P., 2021, Crustal
495 controls on light noble gas isotope variability along the Andean Volcanic Arc: *Geochemical*
496 *Perspectives Letters*.
- 497 Lai, Y., Liu, Y. L., Huang, B. L., and Chen, Y. J., 2005, The characteristics of noble gases in mantle-
498 derived xenoliths in Wudalianchi and Kuandian, NE China: MORB-like mantle and
499 metasomated mantle: *Acta Petrologica Sinica*, v. 21, no. 5, p. 1373-1381.
- 500 Li, Y., Zhang, W., Wang, L., Zhao, F., Han, W., and Chen, G., 2017, Henry's Law and accumulation
501 of crust-derived helium: A case from Weihe Basin, China: *Natural Gas Geoscience*, v. 28, p.
502 495-501.
- 503 Liu, Q., Dai, J., and Jin, Z. J., 2009, Geochemistry and Genesis of Natural Gas in the Foreland and
504 Platform of the Tarim Basin: *Acta Geologica Sinica*, v. 83, p. 107-114.
- 505 Liu, Q., Jin, Z., Chen, J., Krooss, B. M., and Qin, S., 2012, Origin of nitrogen molecules in natural
506 gas and implications for the high risk of N₂ exploration in Tarim Basin, NW China: *Journal of*
507 *Petroleum Science and Engineering*, v. 81, p. 112-121.
- 508 Liu, Q., Liu, W., and Xu, Y., 2007, Geochemistry of natural gas and crude computation of gas-
509 generated contribution for various source rocks in Sulige Gas field, Ordos Basin: *Natural Gas*
510 *Geoscience*, v. 18, p. 697-702.
- 511 Liu, Q., Wu, X., Jia, H., Ni, C., Zhu, J., Miao, J., Zhu, D., Meng, Q., Peng, W., and Xu, H., 2022,
512 Geochemical characteristics of helium in natural gas from the Daniudi gas field, Ordos Basin,
513 central China: *Frontiers in Earth Science*, v. 10, p. 823308.
- 514 Liu, Q., Zhu, D., Jin, Z., Meng, Q., Wu, X., and Hu, H., 2017, Effects of deep CO₂ on petroleum
515 and thermal alteration: The case of the Huangqiao oil and gas field: *Chemical Geology*, v. 469,
516 p. 214-229.
- 517 Liu, Q., Zhu, D., Jin, Z., Tian, H., Zhou, B., Jiang, P., Meng, Q., Wu, X., Xu, H., Hu, T., and Zhu,
518 H., 2023, Carbon capture and storage for long-term and safe sealing with constrained natural
519 CO₂ analogs: *Renewable and Sustainable Energy Reviews*, v. 171, p. 113000.
- 520 Luo, H., Liang, X., Zhang, J., and Yao, Q., 2011, Exploration potential and favorable play
521 identification in the Taizhou low salient of the Subei Basin: *Natural Gas Industry*, v. 31, p. 42-
522 46.
- 523 Ma, J., Tao, M., and Ye, X., 2006, Characteristics and origins of primary fluids and noble gases in
524 mantle-derived minerals from the Yishu area, Shandong Province, China: *Science in China*
525 *Series D*, v. 49, no. 1, p. 77-87.
- 526 Mamyrin, B. A., 1970, Determination of the isotopic composition of astamospheric helium:
527 *Geochemistry International*, v. 7, p. 498-505.
- 528 Marty, B., Jambon, A., and Sano, Y., 1989, Helium isotopes and CO₂ in volcanic gases of Japan:
529 *Chemical Geology*, v. 76, no. 1, p. 25-40.
- 530 Merrill, M. D., Hunt, A. G., and Lohr, C. D., 2014, Noble gas geochemistry investigation of high
531 CO₂ natural gas at the LaBarge Platform, Wyoming, USA: *Energy Procedia*, v. 63, p. 4186-
532 4190.
- 533 Moreira, M., Doucelance, R., Kurz, M. D., Dupré, B., and Allègre, C. J., 1999, Helium and lead
534 isotope geochemistry of the Azores Archipelago: *Earth and Planetary Science Letters*, v. 169,

535 no. 1, p. 189-205.

536 Motyka, R. J., Poreda, R. J., and Jeffrey, A. W., 1989, Geochemistry, isotopic composition, and
537 origin of fluids emanating from mud volcanoes in the Copper River basin, Alaska: *Geochimica*
538 *et Cosmochimica Acta*, v. 53, no. 1, p. 29-41.

539 Mtili, K. M., Byrne, D. J., Tyne, R. L., Kazimoto, E. O., Kimani, C. N., Kasanzu, C. H., Hillegonds,
540 D. J., Ballentine, C. J., and Barry, P. H., 2021, The origin of high helium concentrations in the
541 gas fields of southwestern Tanzania: *Chemical Geology*, v. 585, p. 120542.

542 Ni, C., Wu, X., Liu, Q., Zhu, D., Yang, F., Meng, Q., Xu, H., Xu, S., and Xu, T., 2022, Helium
543 signatures of natural gas from the Dongpu Sag, Bohai Bay Basin, Eastern China: *Frontiers in*
544 *Earth Science*, v. 10, p. 862677.

545 Ni, Y., Dai, J., Tao, S., Wu, X., Liao, F., Wu, W., and Zhang, D., 2014, Helium signatures of gases
546 from the Sichuan Basin, China: *Organic geochemistry*, v. 74, p. 33-43.

547 Nichols, C., Eppink, J., Marquis, M., Alvarado, R., Heidrick, T., DiPietro, P., and Wallace, R., 2014,
548 *Subsurface sources of CO₂ in the Contiguous United States. Volume 1: Discovered Reservoirs.*

549 O'Nions, R. K., and Oxburgh, E. R., 1988, Helium, volatile fluxes and the development of
550 continental crust: *Earth and Planetary Science Letters*, v. 90, no. 3, p. 331-347.

551 Oxburgh, E. R., O'Nions, R. K., and Hill, R. I., 1986, Helium isotopes in sedimentary basins: *Nature*,
552 v. 324, no. 6098, p. 632-635.

553 Poreda, R., and Craig, H., 1989, Helium isotope ratios in circum-Pacific volcanic arcs: *Nature*, v.
554 338, no. 6215, p. 473-478.

555 Poreda, R. J., Jeffrey, A. W. A., Kaplan, I. R., and Craig, H., 1988, Magmatic helium in subduction-
556 zone natural gases: *Chemical Geology*, v. 71, no. 1, p. 199-210.

557 Poreda, R. J., Jenden, P. D., Kaplan, I. R., and Craig, H., 1986, Mantle helium in Sacramento basin
558 natural gas wells: *Geochimica et Cosmochimica Acta*, v. 50, no. 12, p. 2847-2853.

559 Sano, Y., Nakamura, Y., Wakita, H., Urabe, A., and Tominaga, T., 1984, Helium-3 Emission Related
560 to Volcanic Activity: *Science*, v. 224, no. 4645, p. 150-151.

561 Sun, M., Liu, G., and Li, J., 2008, Features of cap rocks of gas pools and criteria of identification:
562 *Natural Gas Industry*, v. 28, p. 36-38.

563 Tao, M., Shen, P., and Xu, Y., 1997a, The characteristic and formation condition of mantle-derived
564 helium accumulations in Subei Basin. : *Natural Gas Geoscience*, v. 8, no. 3, p. 1-8.

565 Tao, M., Xu, Y., and Han, W., 2001, Active characteristics and accumulative effects of mantle-
566 derived fluids in Eastern China.: *Geotectonic et Metallogenia*, v. 25, no. 3, p. 265-270.

567 Tao, M., Xu, Y., Shen, P., and Liu, W., 1997b, Tectonic and geochemical characteristics and reserved
568 conditions of a mantle source gas accumulation zone in Eastern China: *Science in China Series*
569 *D: Earth Sciences*, v. 40, no. 1, p. 73-80.

570 Tao, X., Li, J., Zhao, L., Li, L., Zhu, W., Xing, L., Su, F., Shan, X., Zheng, H., and Zhang, L., 2019,
571 Helium resources and discovery of first supergiant helium reserve in China: Hetianhe Gas field:
572 *Journal of Earth Science*, v. 44, p. 1024-1041.

573 Tedesco, S. A., 2022, *Geology and production of helium and associated gases*, Amsterdam, Elsevier.

574 Umeda, K., Asamori, K., and Kusano, T., 2013, Release of mantle and crustal helium from a fault
575 following an inland earthquake: *Applied geochemistry*, v. 37, p. 134-141.

576 Umeda, K., and Ninomiya, A., 2009, Helium isotopes as a tool for detecting concealed active faults:

577 Geochemistry, Geophysics, Geosystems, v. 10, no. 8, p. Q08010.

578 Wakita, H., and Sano, Y., 1983, $^3\text{He}/^4\text{He}$ ratios in CH_4 -rich natural gases suggest magmatic origin:
579 Nature, v. 305, no. 5937, p. 792-794.

580 Wang, J., Liu, W., Qin, J., Zhang, J., and Shen, B., 2008, Reservoir forming mechanism and origin
581 characteristics in Huangqiao carbon dioxide gas field, North Jiangsu Basin: Natural Gas
582 Geoscience, v. 19, no. 6, p. 827-834.

583 Wang, X., Liu, Q., Liu, W., Zhang, D., Li, X., and Zhao, D., 2022, Accumulation mechanism of
584 mantle-derived helium resources in petroliferous basins, eastern China: Science China Earth
585 Sciences, v. 65, no. 12, p. 2322-2334.

586 Wang, X., Wei, G., Li, J., Chen, J., and Gong, S., 2018, Geochemical characteristics and origins of
587 noble gases of the Kela 2 gas field in the Tarim Basin, China: Marine & Petroleum Geology, v.
588 89, p. 155-163.

589 Wei, G., Wang, D., Wang, X., Li, J., Li, Z., Xie, Z., Cui, H., and Wang, Z., 2014, Characteristics of
590 noble gases in the large Gaoshiti-Moxi gas field in Sichuan Basin, SW China: Petroleum
591 Exploration and Development, v. 41, no. 5, p. 585-590.

592 Wei, L., Lu, X., and Song, Y., 2009, Formation and pool-forming model of CO_2 gas pool in eastern
593 Changde area, Songliao Basin: Petroleum Exploration and Development, v. 36, no. 2, p. 174-
594 180.

595 Xu, D., Zhou, Y., and Zhu, Y., 1999, The $\text{CO}_2/^3\text{He}$ ratio and formation mechanism of mantle-derived
596 CO_2 accumulations in Eastern China.: Oil & Gas Geology, v. 20, p. 290-294.

597 Xu, S., Nakai, S. I., Wakita, H., Xu, Y., and Wang, X., 1995, Helium isotope compositions in
598 sedimentary basins in China: Applied Geochemistry, v. 10, no. 6, p. 643-656.

599 Xu, S., Zheng, G., Zheng, J., Zhou, S., and Shi, P., 2017, Mantle-derived helium in foreland basins
600 in Xinjiang, Northwest China: Tectonophysics, v. 694, p. 319-331.

601 Xu, T., Zhu, H., Feng, G., Yang, Z., and Tian, H., 2019, Numerical simulation of calcite vein
602 formation and its impact on caprock sealing efficiency-Case study of a natural CO_2 reservoir:
603 International Journal of Greenhouse Gas Control, v. 83, p. 29-42.

604 Xu, Y., Liu, W., P., S., and Tao, M., 1998, Geochemistry of noble gases in natural gases, Beijing,
605 Science Press.

606 Xu, Y., Shen, P., Tao, M., and Liu, W., 1996, Geochemistry on mantle-derived volatiles in natural
607 gases from eastern China oil/gas provinces (I): Science in China Series D: Earth Sciences, v.
608 40, no. 2, p. 120-129.

609 Xu, S., Nakai, S., Wakita, H. and Wang, X., 1995. Mantle-derived noble gases in natural gases from
610 Songliao Basin, China. *Geochimica et Cosmochimica Acta*, 1995, v. 59, no. 22), p. 4675-4683.

611 Yakutseni, V. P., 2014, World helium resources and the perspectives of helium industry development:
612 Petroleum Geology, v. 9, no. 1, p. 11.

613 Yang, C., Tao, S., and Hou, L., 2014a, Accumulative Effect of Helium Isotope in Gas Volcanic
614 Reservoirs in Songliao Basin: Natural Gas Geoscience, v. 25, p. 109-115.

615 Yang, F., Wang, J., and Pan, Q., 1991, Discussion on origin of upper Neogene helium-rich gases in
616 Huangqiao, North Jiangsu: Oil & Gas Geology, v. 12, p. 340-345.

617 Yang, G., Li, Y., Ma, X., and Dong, J., 2014b, Effect of Chlorite on CO_2 -water-rock Interaction:
618 Earth Science Frontiers, v. 39, p. 462-472.

- 619 Ye, X., 2003, Enrichment and resource roerground of helium natural gas in Xiqiao area Jiangsu
620 Province: *Jiangsu Geology*, v. 27, p. 207-210.
- 621 Zhang, Y., 2017, Study on sandstone reservoir caharacteristics of Permian Longtan Formation,
622 ineration with CO₂ rich fluid and petroleum accumulation in Huangqiao area, Subei Basin:
623 Nanjing University.
- 624 Zhang, Z., Yang, X., and Cai, H., 2001, Characteristics of basalt reservoir in Minqiao area, Jinhu
625 sag.: *Speical Oil and Gas Reservoirs*, v. 8, no. 3, p. 1-5.
- 626 Zheng, L., Feng, Z., Xu, S., and Liao, Y., 1996, CO₂ gas pools from the earth interior in Jiyang
627 Depression: *Chinese Science Bulletin*, v. 41, no. 8, p. 663-666.
- 628 Zhong, X., 2017, Distribution characteristics and control factors of helium gas in Northern Songliao
629 basin: *Geological Survey and Research*, v. 40, no. 4, p. 300-305.